Physics Letters B 731 (2014) 87–91

Contents lists available at ScienceDirect

Physics Letters B

www.elsevier.com/locate/physletb

Systematic study of elliptic flow parameter in the relativistic nuclear collisions at RHIC and LHC energies

Ben-Hao Sa [a,*], Dai-Mei Zhou [b], Yu-Liang Yan [a], Yun Cheng [b], Bao-Guo Dong [a], Xu Cai [b]

[a] China Institute of Atomic Energy, P.O. Box 275 (10), Beijing 102413, China
[b] Key Laboratory of Quark and Lepton Physics (MOE) and Institute of Particle Physics, Central China Normal University, Wuhan 430079, China

ARTICLE INFO

Article history:
Received 24 October 2013
Received in revised form 30 December 2013
Accepted 10 February 2014
Available online 15 February 2014
Editor: J.-P. Blaizot

ABSTRACT

We employed the new issue of a parton and hadron cascade model PACIAE 2.1 to systematically investigate the charged particle elliptic flow parameter v_2 in the relativistic nuclear collisions at RHIC and LHC energies. With randomly sampling the transverse momentum x and y components of the particles generated in string fragmentation on the circumference of an ellipse instead of circle as originally, the calculated charged particles $v_2(\eta)$ and $v_2(p_T)$ fairly reproduce the corresponding experimental data in the Au+Au/Pb+Pb collisions at $\sqrt{s_{NN}} = 0.2/2.76$ TeV. In addition, the charged particles $v_2(\eta)$ and $v_2(p_T)$ in the p+p collisions at $\sqrt{s} = 7$ TeV as well as in the p+Au/p+Pb collisions at $\sqrt{s_{NN}} = 0.2/5.02$ TeV are predicted.

1. Introduction

To explore the phase transition from the hadronic matter (HM) to quark–gluon matter (QGM) is one of the fundamental aims of relativistic nuclear collisions. A couple years ago, four international collaborations of BRAHMS, PHOBOS, STAR, and PHENIX at RHIC have published white papers [1–4] to declare their evidences for the discovery of strongly coupled quark–gluon plasma (sQGP). One of the most important signals is the large elliptic flow parameter of produced particles in the Au+Au collisions at $\sqrt{s_{NN}} = 200$ GeV.

The measurement of particle elliptic flow parameter v_2 is not trivial. Several methods have been proposed, such as the event plane method [5], Lee–Yang zero point method [6], the cumulant method [7], etc. The cumulant method is even distinguished with two-, four-, and six-particle cumulants. The discrepancy among the v_2 values measured with the event plane method, Lee–Yang zero point method, and the cumulant method may reach a few of tens percent as shown in Figs. 4 and 5 of [8] and Fig. 11 of [9]. Recently, one even argued that the event plane method is obsolete [10].

On the other hand, the particle elliptic flow parameter v_2 is also not easy to investigate theoretically. The conventional (hadronic) transport (cascade) models always underestimated the v_2 experimental data in the nucleus–nucleus collisions at RHIC and/or LHC energies. In [11] it was mentioned that the charged particle v_2 experimental data is around 0.05 in the Au+Au collisions at highest RHIC energy (estimated from $v_2(\eta)$ in [12]), while the UrQMD model provides only half of this value. They have pointed out that a lack of pressure in the model at this energy may be the reason and that the partonic rescattering has to be taken into account in order to describe the data.

Similarly, the default AMPT model (AMPT_*def*) also underestimated the v_2 experimental data in the nucleus–nucleus collisions at RHIC energies [13]. In order to meet with experimental data they updated AMPT_*def* to the AMPT_*sm* with string melting. In the AMPT_*sm* model the hadrons (strings) from HIJING [14] are all melted to the partons. Relying on the rescattering among huge number of partons AMPT_*sm* is able to account for the v_2 experimental data, provided the parton–parton cross section is enlarged to ten mb. Of course, the AMPT_*sm* model has to hadronize the partons after rescattering by the coalescence model rather than the string fragmentation in AMPT_*def*.

In the non-center nucleus–nucleus collisions the geometric overlap zone leads to the initial particle spatial asymmetry distribution. It is then dynamically developed to the final hadronic state transverse momentum asymmetry due to the partonic rescattering [11] and the strong electromagnetic field [15], etc. We have pointed out that the transverse momentum p'_x and p'_y of produced particle from string fragmentation are randomly arranged on a circle with radius of p'_T in the PACIAE 2.0 model [16] (in the PYTHIA model [17] originally). Here the observable with superscript ($'$) refers to the string fragmentation local frame distinguished from the without superscript one referred to the nucleus–nucleus cms frame. This symmetric arrangement strongly cancels the final hadronic state transverse momentum asymmetry developed from the initial spatial asymmetry. In the new issue of a PACIAE model

* Corresponding author.
E-mail address: sabh@ciae.ac.cn (B.-H. Sa).

http://dx.doi.org/10.1016/j.physletb.2014.02.019

(PACIAE 2.1 [18]) we randomly distribute the p'_x and p'_y of produced particle from the string fragmentation on the circumference of an ellipse instead of circle. PACIAE 2.1 is then able to describe the v_2 experimental data.

In the next section, Section 2, a parton and hadron cascade model PACIAE, its new issue of PACIAE 2.1, and the definition of elliptic flow parameter are briefly introduced. The calculated charged particle $v_2(\eta)$ and $v_2(p_T)$ are compared with the corresponding experimental data of the Au+Au/Pb+Pb collisions at $\sqrt{s_{NN}} = 0.2/2.76$ TeV in Section 3. Additionally, the predictions for charged particles $v_2(\eta)$ and $v_2(p_T)$ in the p+p collisions at $\sqrt{s} = 7$ TeV and in the p+Au/p+Pb collisions at $\sqrt{s_{NN}} = 0.2/5.02$ TeV are given in the Section 3. The last section is devoted to the conclusions.

2. Models

The PACIAE model is based on PYTHIA [17]. However, the PYTHIA model is for high energy hadron–hadron (hh) collisions but the PACIAE model is mainly for nucleus–nucleus collisions. In the PYTHIA model a hh collision is decomposed into parton–parton collisions. The hard parton–parton collision is described by the lowest leading order perturbative QCD (LO-pQCD) parton–parton interactions with the modification of parton distribution function in a hadron. The soft parton–parton collision, a non-perturbative process, is considered empirically. The initial- and final-state QCD radiations and the multiparton interactions are also taken into account. So the consequence of a hh collision is a partonic multijet state composed of the diquarks (anti-diquarks), quarks (antiquarks), and the gluons, besides a few hadronic remnants. It is followed by the string construction and fragmentation, thus a final hadronic state is obtained for a hh (pp) collision eventually.

In the PACIAE model [16], the nucleons in a nucleus–nucleus collision are first randomly distributed in the spatial phase space according to the Woods–Saxon distribution. The participant nucleons, resulted from Glauber model calculation, are required to be inside the overlap zone, formed when two colliding nuclei path through each other at a given impact parameter. The spectator nucleons are required to be outside the overlap zone but inside the nucleus–nucleus collision system. Then we decompose a nucleus–nucleus collision into nucleon–nucleon (NN) collisions according to nucleon straight-line trajectories and the NN total cross section. Each NN collision is then dealt by PYTHIA with the string fragmentation switched-off and the diquarks (anti-diquarks) broken into quark pairs (anti-quark pairs). A partonic initial state (composed of the quarks, antiquarks, and the gluons) is obtained for a nucleus–nucleus collision after all of the NN collision pairs were exhausted. This partonic initial stage is followed by a parton evolution stage, where parton rescattering is performed by the Monte Carlo method with $2 \to 2$ LO-pQCD cross sections [19]. The hadronization stage follows the parton evolution stage. The Lund string fragmentation model and a phenomenological coalescence model are provided for the hadronization. However, the string fragmentation model is selected in this calculations. Then the rescattering among produced hadrons is dealt with the usual two body collision model [16]. In this hadronic evolution stage, only the rescatterings among π, K, p, n, $\rho(\omega)$, Δ, Λ, Σ, Ξ, Ω, and their antiparticles are considered for simplicity.

The PACIAE 2.0 model [16] is mainly different from AMPT_*sm* as follows:

1. The partonic initial state is obtained by breaking the strings from PYTHIA in PACIAE 2.0, but by breaking hadrons from HIJING in AMPT_*sm*.
2. The $gg \to gg$ elastic scattering cross section is utilized in the parton rescattering in AMPT_*sm* but specific scattering cross section is used for individual qq (gg) scattering processes in PACIAE 2.0.
3. In the AMPT_*sm* model the partons after rescattering are hadronized by the coalescent model but by string fragmentation in the present PACIAE calculations.

Because of the first difference, the number of initial partons in PACIAE 2.0 is much less than the one in AMPT_*sm*. Hence the strength of partonic rescattering effect in the former is not as strong as that in the later. Therefore relying on partonic rescattering only the PACIAE model is hard to describe v_2 experimental data, unlike AMPT_*sm*. The rearrangement for the transverse momentum x and y components of the particles from string fragmentation, mentioned above, is then required.

The spatial overlap zone formed in non-center nucleus–nucleus collision is almond-like, which is always assumed to be an ellipse with a half-minor axis of $a_r = R_A(1-\delta_r)$ along the x axis (axis of impact parameter) and a half-major axis of $b_r = R_A(1+\delta_r)$ along the y axis (here R_A refers to the radius of nucleus provided a symmetry nucleus–nucleus collisions is considered). Originally this initial spatial asymmetry may develop dynamically into a final hadronic state momentum asymmetry due to the parton rescattering and the strong electromagnetic field, etc. Unfortunately, in the PYTHIA (PACIAE 2.0) model once the transverse momentum p'_T of the produced particle from string fragmentation is randomly sampled according to the exponential and/or Gaussian distribution, its p'_x and p'_y components are randomly arranged on a circle with radius of p'_T, i.e.

$$p'_x = p'_T\cos(\phi'), \qquad p'_y = p'_T\sin(\phi'), \tag{1}$$

where ϕ' refers to the azimuthal angle of particle transverse momentum. This symmetry arrangement strongly cancels the final hadronic state transverse momentum asymmetry developed dynamically from the initial spatial asymmetry. As a prescription to minimize this cancellation, in PACIAE 2.1 [18] we randomly distributed p'_x and p'_y on the circumference of an ellipse with half-major and minor axes of $p'_T(1+\delta_p)$ and $p'_T(1-\delta_p)$, respectively, instead of circle. I.e.

$$p'_x = p'_T(1+\delta_p)\cos(\phi'), \qquad p'_y = p'_T(1-\delta_p)\sin(\phi'). \tag{2}$$

We know from ideal hydrodynamic calculation [20] that the integrated elliptic flow parameter of final hadronic state is approximately proportional to the initial spatial eccentricity of nuclear overlap zone. Therefore we assume that the introduced deformation parameter of δ_p here can be related to the deformation parameter of δ_r in the initial spatial phase space, i.e.

$$\delta_p = C\delta_r \tag{3}$$

where C is an extra model parameter instead of δ_p. We also know that the spatial eccentricity of nucleon distribution in the initial overlap zone, reaction plane eccentricity for instance [21], can be expressed as

$$\begin{aligned}\epsilon_{rp} &= \frac{\sigma_y^2 - \sigma_x^2}{\sigma_y^2 + \sigma_x^2},\\ \sigma_x^2 &= \langle x^2\rangle - \langle x\rangle^2,\\ \sigma_y^2 &= \langle y^2\rangle - \langle y\rangle^2,\end{aligned} \tag{4}$$

where $\langle\cdots\rangle$ denotes the average over the nucleon spatial distribution. This spatial eccentricity should be identical with the geometrical eccentricity [22]

Table 1
Charged particle pseudorapidity densities at mid-rapidity and the fitted model parameters.

Reaction	Energy [TeV]	Experiment	PACIAE	K[a]	β[b]	Δt[c]
		$dN_{ch}/d\eta\|_{mid}$				
p+p (NSD)	0.2	2.25 ± 0.33[d]	2.08	1	0.58	
p+p (NSD)	7	$5.78 \pm 0.01 \pm 0.23$[e]	5.74	2	0.58	
p+Au	0.2		3.63	1	1.7	0.0001
p+Pb (NSD)	5.02	16.81 ± 0.71[f]	16.5	3	0.1	$7 \cdot 10^{-4}$
Au+Au	0.2	640 ± 50[g]	626	1	1.7	0.0001
Pb+Pb	2.76	1612 ± 55[h]	1659	3	0.1	$7 \cdot 10^{-4}$

[a] Correction for the higher order and non-perturbative contributions, default (D) = 1.
[b] A parameter in Lund string fragmentation function, D = 0.58.
[c] Minimum distinguishable collision time interval.
[d] Taken from [24], here NSD refers to the non-single diffractive.
[e] Taken from [25].
[f] Taken from [26].
[g] Taken from [27].
[h] Taken from [28].

$$\epsilon_g = \sqrt{\frac{b_r^2 - a_r^2}{b_r^2}} \tag{5}$$

of the ellipse of initial spatial overlap zone. Using ϵ_{rp} instead of ϵ_g on the left-hand side of Eq. (5) and inserting $b_r = R_A(1+\delta_r)$ as well as $a_r = R_A(1-\delta_r)$ on the right-hand side of Eq. (5), we obtain an algebraic equation of degree 2 in the unknown δ_r

$$\epsilon_{rp}^2 \delta_r^2 + (2\epsilon_{rp}^2 - 4)\delta_r + \epsilon_{rp}^2 = 0. \tag{6}$$

This equation has two analytical roots: The one less than unity is a physical root

$$\delta_r = \frac{2 - \epsilon_{rp}^2 - 2\sqrt{1-\epsilon_{rp}^2}}{\epsilon_{rp}^2}. \tag{7}$$

Another one larger than unity is an unphysical root because δ_r must be $\leqslant 1$. The approximation of

$$\delta_r \simeq \frac{\epsilon_{rp}^2}{4} \tag{8}$$

introduced in PACIAE 2.1 [18] is just a specifically approximated root of Eq. (6). For the p+p and p+A collisions, the weak initial spatial fluctuation (asymmetry) is also possible to be dynamically developed to the final hadronic state transverse momentum asymmetry and the Eq. (3) steamed from hydrodynamic calculation [20] may also be reliable. Just because of the lack of a proper definition for the initial spatial fluctuation (eccentricity ?), we regard δ_p itself as an extra model parameter temporarily.

The Fourier expansion of particle transverse momentum azimuthal distribution reads [5,23]

$$E\frac{d^3N}{d^3p} = \frac{1}{2\pi}\frac{d^2N}{p_T\,dy\,dp_T}\left[1 + \sum_{n=1,2,\ldots} 2v_n \cos\left[n(\phi - \Psi_r)\right]\right], \tag{9}$$

where ϕ refers to the azimuthal angle of particle transverse momentum, Ψ_r stands for the azimuthal angle of reaction plane. In the theoretical study, if the beam direction and impact parameter vector are fixed, respectively, on the p_z and p_x axes in the nucleus–nucleus cms frame, then the reaction plane is just the $p_x - p_z$ plane [23]. Therefore the reaction plane angle, Ψ_r, between the reaction plane and the p_x axis [23] introduced for extracting the elliptic flow experimentally [5] is zero. Eq. (9) and the harmonic coefficients there reduce to

$$E\frac{d^3N}{d^3p} = \frac{1}{2\pi}\frac{d^2N}{p_T\,dy\,dp_T}\left[1 + \sum_{n=1,2,\ldots} 2v_n \cos(n\phi)\right],$$
$$\langle v_n\rangle_p = \langle\cos(n\phi)\rangle_p,$$
$$\langle v_1\rangle_p = \left\langle\frac{p_x}{p_T}\right\rangle_p,$$
$$\langle v_2\rangle_p = \left\langle\frac{p_x^2 - p_y^2}{p_T^2}\right\rangle_p,$$
$$\ldots \tag{10}$$

where $\langle\cdots\rangle_p$ denotes the particle-wise average, i.e. the average over all particles in all events [5].

3. Results and discussions

In the PACIAE 2.1 model simulations, the model parameters are all fixed as the same as default values given in PYTHIA, except the K factor, β, and Δt. They are, respectively, the higher order term corrections for the LO-pQCD parton–parton cross section [17], a factor in the Lund string fragmentation function [17], and the least time interval of two distinguishably consecutive collisions in the partonic initial and evolution stages [16]. These model parameters are first fitted to the experimental data of charged particle pseudorapidity density and are given in Table 1. Later on, these fitted parameters are used in all of the simulations. Additionally, in this study the participant eccentricity [21] of

$$\epsilon_{pa} = \frac{\sqrt{(\sigma_y^2 - \sigma_x^2)^2 + 4\sigma_{xy}^2}}{\sigma_y^2 + \sigma_x^2} \tag{11}$$

is used instead of reaction plane eccentricity ϵ_{rp}. In the above equation σ_{xy} is equal to $\langle xy\rangle - \langle x\rangle\langle y\rangle$. Meanwhile, the physical root of Eq. (7) is employed instead of the specifically approximated root of Eq. (8).

We compare the calculated charged particle $v_2(\eta)$ and $v_2(p_T)$ in the 20–40% and 40–50% central Au+Au collisions at $\sqrt{s_{NN}} = 0.2$ TeV with the corresponding experimental data in the left and right panels of Fig. 1, respectively. The PHENIX data were taken from [29] (using the results of event-plane method). One sees in the left panel that the PACIAE 2.1 results calculated by $C = 2$ well agree with the PHENIX data. The right panel shows that the model results calculated by $C = 1$ reproduce PHENIX data quite well in the $p_T < 3$ GeV/c region. However, the theoretical result decreases with p_T increasing is faster than experimental data in

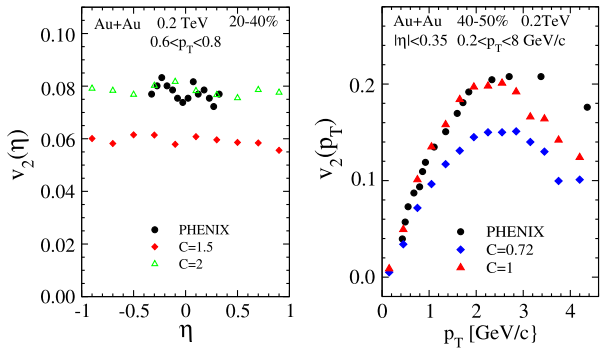

Fig. 1. (Color online.) Charged particle $v_2(\eta)$ (left panel, 20–40% centrality) and $v_2(p_T)$ (right panel, 40–50% centrality) in the Au+Au collisions at $\sqrt{s} = 0.2$ TeV. The PHENIX data were taken from [29] (using the results of event-plane method).

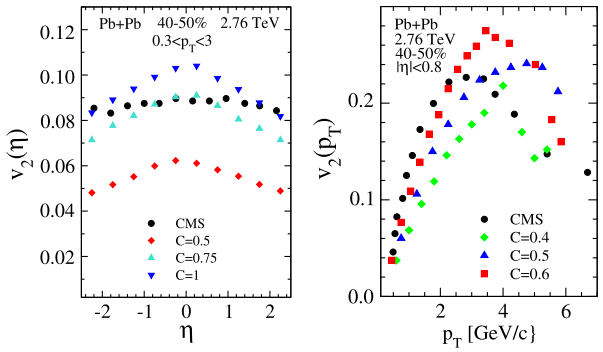

Fig. 2. (Color online.) Charged particle $v_2(\eta)$ (left panel) and $v_2(p_T)$ (right panel) in the Pb+Pb collisions at $\sqrt{s} = 2.76$ TeV. The CMS data are taken from [9] (using results of the Lee–Yang zero point method for $v_2(\eta)$ and the event-plane method for $v_2(p_T)$).

the $p_T > 3$ GeV/c region. As most of particles are generated below $p_T \sim 2$ TeV/c (about 95 percent of the total multiplicity), one always satisfies the agreement between model calculations and experimental data within $p_T \leqslant 2$ GeV/c, cf. Fig. 7 in the first quotation of Ref. [13] for instance. As for the best model parameter $C \sim 2$ in the left panel but 1 in the right panel, which may be attributed to the difference in the studied centrality bin, 20–40% in former but 40–50% in the later. Thus the centrality dependence of parameter C should be studied later.

Similarly, the calculated charged particle $v_2(\eta)$ and $v_2(p_T)$ in the 40–50% central Pb+Pb collisions at $\sqrt{s_{NN}} = 2.76$ TeV are compared with the corresponding CMS data [9] (using the results of Lee–Yang zero point method for $v_2(\eta)$ and event-plane method for $v_2(p_T)$) in Fig. 2. We see in this figure that the PACIAE 2.1 model is also able to describe the CMS data by adjusting the extra parameter C.

In the Figs. 3, 4, and 5 we give the PACIAE 2.1 model predictions for the charged particle $v_2(\eta)$ and $v_2(p_T)$ in the minimum bias (MB) p+Au and p+Pb, as well as in the non-single diffractive (NSD) p+p collisions at $\sqrt{s_{NN}} = 0.2, 5.02,$ and 7 TeV, respectively. We see in these figures that the elliptic flow parameter may reach a amount of 0.04, 0.07, and 0.016 (estimated from $v_2(\eta)$) in the p+Au, p+Pb, and p+p collisions at $\sqrt{s_{NN}} = 0.2, 5.02,$ and 7 TeV, respectively. This amount of the elliptic flow parameter may be measurable experimentally. One sees in Fig. 5 that v_2 seems to be proportional to the value of deformation parameter δ_p in the p+p collisions. However, the behavior of $v_2(\eta)$ and $v_2(p_T)$ changing with δ_p is needed to be further investigated in detail.

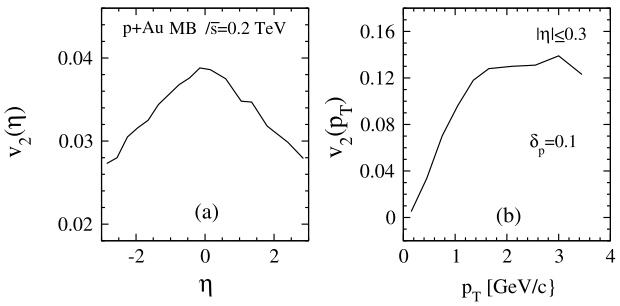

Fig. 3. Predicted charge particle $v_2(\eta)$ (panel (a)) and $v_2(p_T)$ (panel (b)) in the p+Au collisions at $\sqrt{s_{NN}} = 0.2$ TeV ($\delta_p = 0.1$).

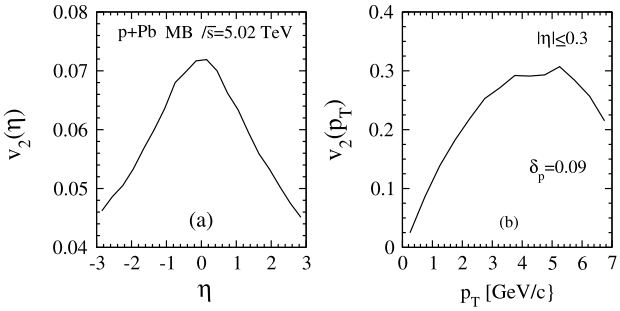

Fig. 4. Predicted charge particle $v_2(\eta)$ (panel (a)) and $v_2(p_T)$ (panel (b)) in the p+Pb collisions at $\sqrt{s_{NN}} = 5.02$ TeV ($\delta_p = 0.09$).

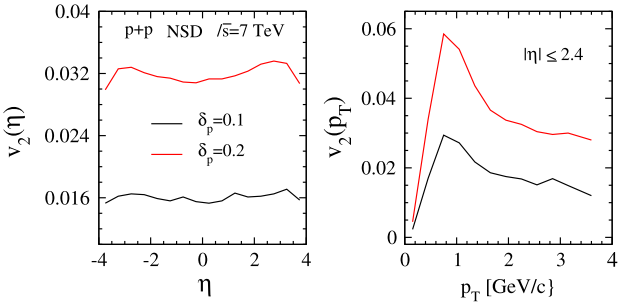

Fig. 5. (Color online.) Predicted charge particle $v_2(\eta)$ (left panel) and $v_2(p_T)$ (right) in the p+p collisions at $\sqrt{s} = 7$ TeV.

4. Conclusions

In summary, we have employed the new issue of a parton and hadron cascade model PACIAE 2.1 investigating systematically the charged particle elliptic flow parameter v_2 in the relativistic nuclear collisions at RHIC and LHC energies. Because of the new introduced mechanism of random arrangement of the particles from string fragmentation on the circumference of an ellipse instead of circle originally, the calculated charge particle $v_2(\eta)$ and $v_2(p_T)$ in the Au+Au/Pb+Pb collisions at $\sqrt{s_{NN}} = 0.2/2.76$ TeV describe the corresponding experimental data fairly well. Meanwhile, the charged particle $v_2(\eta)$ and $v_2(p_T)$ in the p+Au/p+Pb collisions at $\sqrt{s_{NN}} = 0.2/5.02$ TeV and in the p+p collisions at $\sqrt{s} = 7$ TeV are predicted. The elliptic flow parameter in these reactions reaches a measurable amount.

As mentioned in the first section that the elliptic flow parameter is important observable relevant to the exploring of sQGP. However, the measurement of v_2 is not trivial. The discrepancy among v_2 values measured by the event plane method [5], Lee–Yang zero point method [6], and the cumulant method [7] may reach a few ten percent as shown in Figs. 4 and 5 of [8] and Fig. 11 of [9]. On the other hand, the obscures also exist among the

various v_2 model calculations as mentioned in the first section. So the further studies for v_2 asymmetry are still required both experimentally and theoretically.

This work is just a first step along the novel approach. Further investigations, such as the cross section effect, energy and centrality dependence of C parameter, as well as the detail study for the dependence of $v_2(p_T)$ and $v_2(\eta)$ on δ_p (C), are really required.

Acknowledgements

This work was supported by the National Natural Science Foundation of China under grant Nos. 11075217, 11105227, 11175070, 11477130, and by the 111 Project of the Foreign Expert Bureau of China. B.H.S. would like to thank Zi-Wei Lin for discussions. Y.L.Y. acknowledges the financial support from SUT-NRU project under contract No. 17/2555.

References

[1] I. Arsene, et al., BRAHMS Collaboration, Nucl. Phys. A 757 (2005) 1.
[2] B.B. Back, et al., PHOBOS Collaboration, Nucl. Phys. A 757 (2005) 28.
[3] J. Admas, et al., STAR Collaboration, Nucl. Phys. A 757 (2005) 102.
[4] K. Adcox, et al., PHENIX Collaboration, Nucl. Phys. A 757 (2005) 184.
[5] A.M. Poskanzer, S.A. Voloshin, Phys. Rev. C 58 (1998) 1671.
[6] R.S. Bhalerao, N. Borghini, J.-Y. Ollitrault, Nucl. Phys. A 727 (2003) 373.
[7] N. Borghini, P.M. Dinh, J.-Y. Ollitrault, Phys. Rev. C 63 (2001) 054906.
[8] B.I. Abelev, et al., STAR Collaboration, Phys. Rev. C 77 (2008) 054901.
[9] CMS Collaboration, Phys. Rev. C 87 (2013) 014902, arXiv:1204.1409v1 [nucl-ex].
[10] M. Luzum, J.-Y. Ollitrault, arXiv:1209.2323v2 [nucl-ex].
[11] H. Peterson, M. Bleicher, Eur. Phys. J. C 49 (2007) 91.
[12] B.B. Back, et al., Phys. Rev. Lett. 94 (2005) 122303.
[13] Zi-wei Lin, C.M. Ko, Phys. Rev. C 65 (2002) 034904;
Zi-wei Lin, C.M. Ko, Phys. Rev. C 72 (2005) 064901.
[14] X.N. Wang, M. Gyulassy, Phys. Rev. D 44 (1991) 3501.
[15] K. Tuchin, arXiv:1301.0099v1 [hep-ph].
[16] Ben-Hao Sa, Dai-Mei Zhou, Yu-Liang Yan, Xiao-Mei Li, Sheng-Qin Feng, Bao-Guo Dong, Xu Cai, Comput. Phys. Commun. 183 (2012) 333.
[17] T. Sjöstrand, S. Mrenna, P. Skands, J. High Energy Phys. 0605 (2006) 026.
[18] Ben-Hao Sa, Dai-Mei Zhou, Yu-Liang Yan, Bao-Guo Dong, Xu Cai, Comput. Phys. Commun. 184 (2013) 1476.
[19] B.L. Combridge, J. Kripfgang, J. Ranft, Phys. Lett. B 70 (1977) 234.
[20] P.F. Kolb, J. Sollfrank, U.W. Heinz, Phys. Rev. C 62 (2000) 054909.
[21] B. Alver, et al., Phys. Rev. C 77 (2008) 014906.
[22] W.H. Beyer, Standard Mathematical Tables and Formulae, 29th edition, CRC Press, London, 2000, p. 177.
[23] S.A. Voloshin, Y. Zhang, Z. Phys. C 70 (1996) 665.
[24] PHOBOS Collaboration, Phys. Rev. C 83 (2011) 024913.
[25] CMS Collaboration, Phys. Rev. Lett. 105 (2010) 022002.
[26] ALICE Collaboration, Phys. Rev. Lett. 110 (2013) 032301, arXiv:1210.3615v1 [nucl-ex].
[27] PHOBOS Collaboration, Phys. Rev. Lett. 91 (2003) 052303.
[28] CMS Collaboration, J. High Energy Phys. 1108 (2011) 141, arXiv:1107.4800v2 [nucl-ex].
[29] S. Afanasiev, et al., PHENIX Collaboration, Phys. Rev. C 80 (2003) 024909.